Experimental preparation of Greenberger-Horne-Zeilinger states in an Ising spin model by partially suppressing the nonadiabatic transitions

Yunlan Ji,[1,2] Ji Bian,[1,2] Xi Chen,[1,2] Jun Li,[3] Xinfang Nie,[3] Hui Zhou,[4,*] and Xinhua Peng[1,2,5,†]

[1]*Hefei National Laboratory for Physical Sciences at the Microscale and Department of Modern Physics, University of Science and Technology of China, Hefei 230026, China*

[2]*CAS Key Laboratory of Microscale Magnetic Resonance, University of Science and Technology of China, Hefei, Anhui 230026, China*

[3]*Department of Physics and Shenzhen Institute for Quantum Science and Engineering, Southern University of Science and Technology, Shenzhen 518055, China*

[4]*Department of Physics, Shaanxi University of Science and Technology, Xi'an 710021, China*

[5]*Synergetic Innovation Center of Quantum Information and Quantum Physics, University of Science and Technology of China, Hefei, Anhui 230026, China*

(Received 19 January 2019; published 15 March 2019)

The creation of multipartite entangled states is a key task of quantum information processing. Among the various implementations, shortcut to adiabaticity (STA) offers a fast and robust means for generating entanglement. The traditional counterdiabatic driving, as a conventional and simple method for STA, suppresses transitions with an auxiliary Hamiltonian, but its complex interactions in many-body systems may hamper the feasibility of experimental implementation. To avoid this drawback, a flexible and efficient way was proposed theoretically by Chen *et al.* [Phys. Rev. A **93**, 052109 (2016)] by substituting the counterdiabatic terms. Inspired by this work, we devise a practical protocol for preparing the Greenberger-Horne-Zeilinger state on the Ising spin model via STA by partial suppression of the nonadiabatic transitions, which can obviously reduce the complexity in experiments compared with the original method. We also experimentally demonstrate the viability of our scheme with a nuclear magnetic resonance quantum simulator. This work provides an alternative method to realize fast coherent quantum control for a multiqubit system in experiments.

DOI: 10.1103/PhysRevA.99.032323

I. INTRODUCTION

Entanglement is one of the fundamental signatures of quantum physics, which stays at the heart of diverse applications ranging from quantum computation to quantum teleportation and quantum cryptography [1–4]. Besides, it plays a crucial role in a broad range of phenomena encompassing many-body physics, e.g., the fractional quantum Hall effect [5] and quantum phase transitions [6]. Recently, various methods of preparing entangled states, such as global control method [7,8], quantum network method [9,10], adiabatic method [11,12], and dissipative method [13,14], have been proposed and demonstrated in theory and experiments. Due to good robustness against weak variations of the system, the adiabatic passage has been one of the mostly used methods in experiments. However, a common shortcoming of this scheme is that a high-fidelity target state is typically achieved at the cost of time. This may lead to a conflict between the time required by the adiabatic theorem and decoherence time.

To alleviate this disadvantage, Demirplack and Rice in Ref. [15], and Berry in Ref. [16] proposed a novel method to accelerate adiabatic protocols by supplementing the original Hamiltonian with an auxiliary counterdiabatic driving (CD) term H_{cd}, which can reach the same goal as adiabatic evolutions without constrains on the evolution time. After that, an emergent field, namely shortcut to adiabaticity (STA), aiming at speeding up the quantum adiabatic process has attracted much interest and a variety of shortcut protocols have been developed, to name a few, counterdiabatic driving [17] or transitionless quantum driving, invariant-based inverse engineering [18,19], and fast-forward methods [20,21]. By now, the STA idea has been successfully extended to non-Hermitian [22,23] and open quantum systems [24,25], and has found applications in a wide range of fields such as many-body physics and quantum science and technologies [26–38].

As one of the most successful strategies for STA, counterdiabatic driving provides a quite simple way to precisely suppress nonadiabatic transitions between instantaneous eigenstates. However, the time-dependent term H_{cd} typically suffers from complex many-body interactions with the growth of the system. This leads to the difficulty in ensuring transitionless evolution with the available experimental controls [39–42], and much effort has been devoted to address this issue [43–45]. For example, in cavity QED systems a complicated Hamiltonian can be simplified with the help of quantum Zeno dynamics and then the STA for quantum state preparation was constructed with an effective Hamiltonian [46].

Recently, Chen *et al.* presented an available method for constructing STA in theory by a substitute of CD term [47], which can achieve a precise and flexible control of speed-up protocols in both Hermitian and non-Hermitian systems because of the multiple choices for designing additional terms.

*zhouhui@sutc.edu.cn
†xhpeng@ustc.edu.cn

Motivated by this method, here we put forward a scheme on the Ising system to prepare the Greenberger-Horne-Zeilinger (GHZ) state $|\Psi\rangle = (|0\rangle^{\otimes N} + |1\rangle^{\otimes N})/\sqrt{2}$, which is one of the key resources in the field of quantum metrology for quantum-mechanically enhanced sensors, with measurement precision approaching the Heisenberg limit $1/N$ [48,49]. The GHZ state is also at the core of Schrödinger's cat paradox for its novel nonlocal property. The rest of the paper is organized as follows. In Sec. II we concisely review the theory of designing transitionless evolutions without directly using the CD term. In Sec. III, an application of this method to create GHZ state is presented on a three-spin Ising system. Sec. IV provides a proof-of-principle experiment using a three-qubit nuclear magnetic resonance (NMR) quantum simulator. Finally, a brief summary with a discussion is presented in Sec. V.

II. REVIEW OF THE METHOD TO CONSTRUCT STA WITH SUBSTITUTIVE CD TERM

For an arbitrary time-dependent quantum Hamiltonian $H_0(t)$, the instantaneous eigenenergies $E_n(t)$ and eigenstates $|\phi_n(t)\rangle$ are given by

$$H_0(t)|\phi_n(t)\rangle = E_n(t)|\phi_n(t)\rangle, \tag{1}$$

in which the instantaneous eigenstates satisfy the orthogonal completeness relation: $\langle\phi_n(t)|\phi_m(t)\rangle = \delta_{nm}$, and $\sum_n |\phi_n(t)\rangle\langle\phi_n(t)| = I$. If the variation of Hamiltonian H_0 is slow enough to satisfy the adiabatic approximation $|\langle\phi_m(t)|\partial_t H_0|\phi_n(t)\rangle|/[E_n(t) - E_m(t)]^2 \ll 1$, the system will stay at an instantaneous eigenstate, and the quantum transitions will be suppressed. Otherwise, undesirable quantum transitions will take place due to nonadiabatic changes of the Hamiltonian.

Berry [16] found a formula of the driving Hamiltonian where no unwanted transitions occur if the system is subject to a combined time-dependent Hamiltonian $H(t) = H_0(t) + H_{cd}(t)$, with

$$H_{cd}(t) = i\hbar \sum_n |\dot{\phi}_n(t)\rangle\langle\phi_n(t)|. \tag{2}$$

The overdot here means time derivative. However, $H_{cd}(t)$ usually includes many-body interactions and the complexity increases as system size grows. Consequently, one may be unable to directly construct the required form of $H_{cd}(t)$ in experiments. Reference [47] provides a simple method to find a substitute Hamiltonian $H_{add}(t)$ to avoid the mentioned drawback. A brief explanation of the idea is as follows.

The dynamics of a system governed by Hamiltonian $H_0(t)$ is described by the Shrödinger equation:

$$i\hbar\partial_t|\psi(t)\rangle = H_0(t)|\psi(t)\rangle. \tag{3}$$

The time-dependent $|\psi(t)\rangle$ can be expressed as $|\psi(t)\rangle = \sum_n a_n(t)|\mu_n\rangle = [a_1(t), a_2(t), \ldots, a_n(t)]^t$, with $\{a_n(t)\}$ being the probability amplitudes of all the bare states expanded by a collective basis set $\{|\mu_n\rangle\}$. This basis set also satisfies the orthogonal completeness relation, i.e., $\sum_n |\mu_n\rangle\langle\mu_n| = I$, $\langle\mu_m|\mu_n\rangle = \delta_{mn}$, and therefore $|\mu_m\rangle\langle\mu_n| = M_{m,n}$ denotes a matrix whose elements are all zero except that the mth row and the nth column are 1.

In the basis of instantaneous eigenstates of $H_0(t)$, namely in the eigenpicture, the system dynamics can be also described by the Schrödinger equation

$$i\hbar\partial_t|\psi^e(t)\rangle = H_0^e(t)|\psi^e(t)\rangle, \tag{4}$$

where the superscript e indicates the wave function written in the eigenpicture and $|\psi^e(t)\rangle = [c_1(t), c_2(t), \ldots, c_n(t)]^t$. The transformation between the Schrödinger picture and eigenpicture satisfies the formula $|\psi^e(t)\rangle = R^\dagger|\psi(t)\rangle$ with the operator $R^\dagger = \sum_{m,n} M_{m,n}\langle\phi_m|\mu_n\rangle = \sum_m |\mu_m\rangle\langle\phi_m|$. Then, according to Eq. (3) and Eq. (4), we obtain

$$H_0^e(t) = R^\dagger H_0 R - i\hbar R^\dagger \dot{R}, \tag{5}$$

where $R^\dagger H_0 R = \sum_n M_{n,n}E_n$ is the diagonalization matrix for $H_0(t)$, and

$$\begin{aligned} i\hbar R^\dagger\dot{R} = {} & i\hbar \sum_n M_{n,n}\langle\phi_n(t)|\dot{\phi}_n(t)\rangle \\ & + i\hbar \sum_{n\neq m} M_{n,m}\langle\phi_n(t)|\dot{\phi}_m(t)\rangle. \end{aligned} \tag{6}$$

The integral of the first term in Eq. (6) is the adiabatic phase, and the second term is the nonadiabatic coupling. If we add the term $H_1^e(t) = i\hbar R^\dagger\dot{R}$ to Eq. (5), i.e., just the CD term in the Schrödinger picture, the undesired transitions can be completely suppressed. This term typically requires time-dependent control of complex interactions and the implementation of H_{cd} is often a tough work. Provided that there exists an available Hamiltonian $H_{add}(t) = \sum_{k,l} M_{k,l}A_{kl}$ with A_{kl} being the time-dependent coefficient, then by adding this Hamiltonian into Eq. (5) we obtain

$$H^e(t) = H_0^e + R^\dagger H_{add} R, \tag{7}$$

where $R^\dagger H_{add} R = \sum_{n,m,k,l} M_{n,m}\phi_{nk}^*\phi_{ml}A_{kl}$, and ϕ_{nm} denotes the mth element of the column vector $|\phi_n(t)\rangle$. Once $R^\dagger H_{add} R$ nullifies the nonadiabatic coupling term $i\hbar\sum_{n\neq m} M_{n,m}\langle\phi_n(t)|\dot{\phi}_m(t)\rangle$, that is,

$$\sum_{k,l} \phi_{nk}^*\phi_{ml}A_{kl} = i\hbar\langle\phi_n(t)|\dot{\phi}_m(t)\rangle, \quad n \neq m, \tag{8}$$

the shortcuts can be constructed. Furthermore, even if part of the transitions are suppressed, the shortcuts remain effective. With the advantage of flexibility in constructing the available STA in practice, an example application of this method to produce the GHZ state is presented as follows.

III. APPLICATION IN GHZ STATE PREPARATION

The Ising model is ubiquitous in many physical systems and plays an important role in both condensed-matter physics and quantum computation [50–56]. Consider a three-spin Ising model in an external magnetic field:

$$H_0(t) = -B(t)\sum_{i=1}^N \sigma_x^i - J(t)\sum_{i=1}^N \sigma_z^i\sigma_z^{i+1} \tag{9}$$

with periodic boundary condition, i.e., $\sigma_v^{N+1} = \sigma_v^1$ and $N = 3$. Here $B(t)$ and $J(t)$ denote time-dependent magnetic field and spin-spin couplings strength respectively, and $\sigma_{v(v=x,y,z)}^i$ denote the Pauli operators of the ith qubit.

It turns out that we can adiabatically drive the system from the product state $[|0\rangle+|1\rangle]^{\otimes 3}$ to the GHZ state by switching from $B \gg J$ to $B \ll J$. For simplicity, we set $\hbar = 1, J(t) = \sin\gamma$ and $B(t) = \cos\gamma$ with the time-dependent parameter $\gamma(t) \in [0, \pi/2]$. Thus the instantaneous eigenvalues of $H_0(t)$ are $\mathcal{E}_{1,2}(t) = \sin\gamma - \cos\gamma$, $\mathcal{E}_{3,4}(t) = \sin\gamma + \cos\gamma$, $\mathcal{E}_{5,6}(t) = -\cos\gamma - \sin\gamma \mp \sqrt{4 - 2\sin 2\gamma}$, and $\mathcal{E}_{7,8}(t) = \cos\gamma - \sin\gamma \mp \sqrt{4 + 2\sin 2\gamma}$. The corresponding first four time-independent eigenstates can be given as $|\phi_{1,3}\rangle = [\mp|001\rangle - |011\rangle \pm |100\rangle + |110\rangle]/2$, $|\phi_{2,4}\rangle = [\mp|010\rangle - |011\rangle \pm |100\rangle + |101\rangle]/2$, and the other four time-dependent eigenvectors are

$$
\begin{aligned}
|\phi_5(t)\rangle &= \frac{\cos\eta_-}{\sqrt{2}}[|000\rangle + |111\rangle] + \frac{\sin\eta_-}{\sqrt{2}}[|W\rangle + \overline{|W\rangle}],\\
|\phi_6(t)\rangle &= \frac{\sin\eta_-}{\sqrt{2}}[|000\rangle + |111\rangle] - \frac{\cos\eta_-}{\sqrt{2}}[|W\rangle + \overline{|W\rangle}],\\
|\phi_7(t)\rangle &= \frac{\cos\eta_+}{\sqrt{2}}[|111\rangle - |000\rangle] - \frac{\sin\eta_+}{\sqrt{2}}[|W\rangle - \overline{|W\rangle}],\\
|\phi_8(t)\rangle &= \frac{\sin\eta_+}{\sqrt{2}}[|111\rangle - |000\rangle] + \frac{\cos\eta_+}{\sqrt{2}}[|W\rangle - \overline{|W\rangle}],
\end{aligned}
$$

where $\overline{|W\rangle} = \sigma_x^{\otimes 3}|W\rangle = \frac{1}{\sqrt{3}}(|011\rangle+|110\rangle+|101\rangle)$, and $\tan\eta_\pm = (1 \pm 2\tan\gamma \mp 2\sqrt{\sec^2\gamma \pm \tan\gamma})/\sqrt{3}$. When $\gamma(t)$ adiabatically changes from 0 to $\pi/2$, the ground state $|\phi_5(t)\rangle$ can reach GHZ state. The time duration, to guarantee that no excitation occurs, depends on the adiabatic condition.

To accelerate the adiabatic process, according to Eq. (2) the exact CD term can be calculated as:

$$
\begin{aligned}
H_{cd}(t) = &-\frac{\dot\gamma}{7+\cos 4\gamma}\sum_{i\neq j} p\big(\sigma_z^i\sigma_y^j\big)\\
&-\frac{\dot\gamma\sin 2\gamma}{14+2\cos 4\gamma}\sum_{i\neq j\neq k} p\big(\sigma_x^i\sigma_y^j\sigma_z^k\big),
\end{aligned}
\tag{10}
$$

where $p(\cdot)$ denotes a permutation of the individual spin. In theory, the adiabatic evolution can be realized in a finite duration by directly adding the term $H_{cd}(t)$ to $H_0(t)$. However, such a complicated term involves six two-body interactions and six three-body interactions. What's more, inherent multi-body interaction is absent in NMR, we have to simulate it with many radio-frequency pulses and two-body interactions [57]. Therefore, errors accumulated from the decoherence effect and imperfect operations will increase the difficulties in experiments.

As demonstrated in Ref. [47], once the nonadiabatic coupling terms are nullified partially, the traditional CD term $H_{cd}(t)$ can be replaced by Hamiltonian $H_{add}(t)$ for speeding up the adiabatic process. The transformation matrix between the Schrödinger picture and eigenpicture is given as $R(t) = \sum_{m=1}^{8}|\phi_m(t)\rangle\langle\mu_m|$. Then,

$$
iR^\dagger\dot R = i\dot\gamma\left(\frac{\sqrt{3}(M_{6,5}-M_{5,6})}{4-2\sin 2\gamma} + \frac{\sqrt{3}(M_{8,7}-M_{7,8})}{4+2\sin 2\gamma}\right),
$$

which represents the transitions $|\phi_5(t)\rangle \leftrightarrow |\phi_6(t)\rangle$ and $|\phi_7(t)\rangle \leftrightarrow |\phi_8(t)\rangle$. The designed term $H_{add}(t) = \sum_{m,n} M_{m,n}A_{mn}(t)$ can be employed to suppress these transitions by solving Eq. (8) theoretically. But this is a tough task because of a severe amount of computation needed to do with the 8×8 parameters. To ensure the feasibility of the subsequent experiment, we can adopt a set of controllable operators h_k in experiments. Here only two-body interactions in this system, i.e., $\{h_1 = \sigma_z^1\sigma_y^2,\ h_2 = \sigma_y^1\sigma_z^2,\ h_3 = \sigma_z^2\sigma_y^3,\ h_4 = \sigma_y^2\sigma_z^3,\ h_5 = \sigma_z^3\sigma_y^1,\ h_6 = \sigma_y^3\sigma_z^1\ \}$, are used to design shortcut to adiabatic passage. The additional Hamiltonian is expressed as

$$
H_{add}(t) = -\sum_{k=1}^{N}\alpha_k(t)h_k, \tag{11}
$$

where $\alpha_k(t)$ denotes the coupling strength and N is the number of the operators.

Let us take a look at some properties of this system before we move on. The Hamiltonians $H_0(t)$ and $H_{add}(t)$ commute with the operator $X = \prod_{i=1}^{3}\sigma_x^i$, so that these two Hamiltonians can be simultaneously block diagonalized in the two eigenspaces $\mathcal{X}_{\pm 1}$ of X with eigenvalues ± 1, and the eight eigenstates of $H_0(t)$ belong to different subspaces, i.e.,

$$
\{|\phi_3\rangle, |\phi_4\rangle, |\phi_5(t)\rangle, |\phi_6(t)\rangle\} \in \mathcal{X}_{+1},
$$

and

$$
\{|\phi_1\rangle, |\phi_2\rangle, |\phi_7(t)\rangle, |\phi_8(t)\rangle\} \in \mathcal{X}_{-1}.
$$

Therefore any initial state in one of the two orthogonal invariant subspaces, driven by $H_0(t) + H_{add}(t)$, would remain in such a subspace. Here we only need to suppress the transitions between the state $|\phi_5(t)\rangle$ and other excited states in the subspace $\mathcal{X}_{+1}$, i.e., $|\phi_5(t)\rangle \leftrightarrow \{|\phi_3(t)\rangle, |\phi_4(t)\rangle, |\phi_6(t)\rangle\}$. According to Eq. (8), we obtained a set of homogeneous linear equations as follows:

$$
\begin{aligned}
\sqrt{3}(\alpha_2-\alpha_3+\alpha_5-\alpha_6)\cos\eta_- + (2\alpha_1+\alpha_2-\alpha_3-2\alpha_4-\alpha_5+\alpha_6)\sin\eta_- &= 0,\\
\sqrt{3}(\alpha_1-\alpha_2+\alpha_4-\alpha_5)\cos\eta_- + (\alpha_2-\alpha_1+2\alpha_3+\alpha_4-\alpha_5-2\alpha_6)\sin\eta_- &= 0,\\
\alpha_1+\alpha_2+\alpha_3+\alpha_4+\alpha_5+\alpha_6 - 3\dot\gamma/(4-2\sin 2\gamma) &= 0,
\end{aligned}
\tag{12}
$$

where the time-dependent parameter η_- has been defined above. These equations are used to partially nullify the nonadiabatic coupling terms and accelerate the adiabatic protocol. Since the rank of the coefficient matrix of the above equations is less than the number of variables, the solution is not unique. But in practical situations, it would be reasonable to set some of the parameters as zero.

TABLE I. Solutions to Eqs. (12) on the condition that any several variables are set to be zero. Here the time-dependent parameter $\eta_-(t) = \arctan\left([1 - 2\tan\gamma(t) + 2\sqrt{\sec^2\gamma(t) - \tan\gamma(t)}]/\sqrt{3}\right)$.

1.	$\alpha_1 = \alpha_3 = \alpha_4 = 0$	$\alpha_2 = \frac{\dot\gamma(3+\sqrt{3}\cot\eta_-)}{8-4\sin 2\gamma}$;	$\alpha_5 = \frac{3\dot\gamma\csc 2\eta_-}{(4-2\sin 2\gamma)(\tan\eta_- - \sqrt{3})}$;	$\alpha_6 = \frac{3\dot\gamma}{(2-\sin 2\gamma)(3-\sqrt{3}\tan\eta_-)}$	
2.	$\alpha_1 = \alpha_3 = \alpha_6 = 0$	$\alpha_2 = \frac{\dot\gamma(3-\sqrt{3}\cot\eta_-)}{8-4\sin 2\gamma}$;	$\alpha_4 = \frac{3\dot\gamma}{(2-\sin 2\gamma)(3+\sqrt{3}\tan\eta_-)}$;	$\alpha_5 = \frac{3\dot\gamma\csc 2\eta_-}{(4-2\sin 2\gamma)(\sqrt{3}+\tan\eta_-)}$	
3.	$\alpha_2 = \alpha_4 = \alpha_6 = 0$	$\alpha_1 = \alpha_3 = \alpha_5 = \frac{\dot\gamma}{4-2\sin 2\gamma}$			
4.	$\alpha_1 = \alpha_3 = \alpha_5 = \alpha_6 = 0$	$\alpha_2 = \frac{\dot\gamma(3+\sqrt{3}\tan\eta_-)}{8-4\sin 2\gamma}$;	$\alpha_4 = \frac{\dot\gamma(3-\sqrt{3}\tan\eta_-)}{8-4\sin 2\gamma}$		
...	...	...			

To get a unique solution of these equations, three out of the six variables are chosen to be zero, and the rationality will be subsequently proved. Although there are many groups under such condition, the premise should be that the coefficients $\alpha_k(t)$ are finite and smooth functions. A series of solutions are shown in Table I and plotted in Fig. 1. Here a linear evolution is given by $\gamma(t) = \frac{\pi t}{2T}$, and the total duration $T = 1$ for simplicity. In Figs. 1(a) and 1(b), we can see that some couplings tend to infinity near the boundary, which is not available in experiment and these solutions have to be ruled out.

A special case is obtained by imposing a constraint that $\alpha_{2,4,6} = 0$, and the other parameters $\alpha_{1,3,5}(t) = \alpha_{add}(t)$, and

$$\alpha_{add}(t) \equiv \frac{\dot\gamma}{4 - 2\sin 2\gamma}. \tag{13}$$

The result illustrated in Fig. 1(c) shows that parameters are available in experiment. To further validate the feasibility, we calculate the fidelity of the state $|\Phi(t)\rangle$ driven along the constructed Hamiltonian $H(t) = H_0(t) + H_{add}(t)$ with $H_{add}(t) = -\alpha_{add}(t)(h_1 + h_3 + h_5)$. The fidelity here is defined as $F(t) = |\langle \mathrm{GHZ}|\Phi(t)\rangle|^2$ and tends to 1 quickly (orange squares) as depicted in Fig. 2, which has the same effect as the CD scheme $H_0(t) + H_{cd}(t)$ (red solid line). By contrast, the final fidelity is only about 0.63 without any additional terms (black dashed line). As we can see the number of many-body interactions is greatly reduced; the target state, which has the same precision as the traditional CD method, can be prepared with reduced complexity in practice.

A matter of effectiveness may appear, if the number of the operators h_k is further reduced. Notice that the Eqs. (12) represent the suppression on transitions $|\phi_5(t)\rangle \leftrightarrow \{|\phi_3(t)\rangle, |\phi_4(t)\rangle, |\phi_6(t)\rangle\}$, respectively. It is reasonable to believe that even if only part of the equations take effect, the constructed shortcut will also work. For example, if $\alpha_{1,3,5,6} = 0$ the other parameters $\alpha_{2,4}(t)$ can be acquired through the second and third equations in Eqs. (12) as presented in Fig. 1(d) and Table I (fourth row). Driven by this Hamiltonian $H'(t) = H_0(t) + H'_{add}(t)$ with $H'_{add}(t) = -\alpha_2(t)h_2 - \alpha_4(t)h_4$, the final fidelity gets close to 83% as shown in Fig. 2 (blue dashed line),

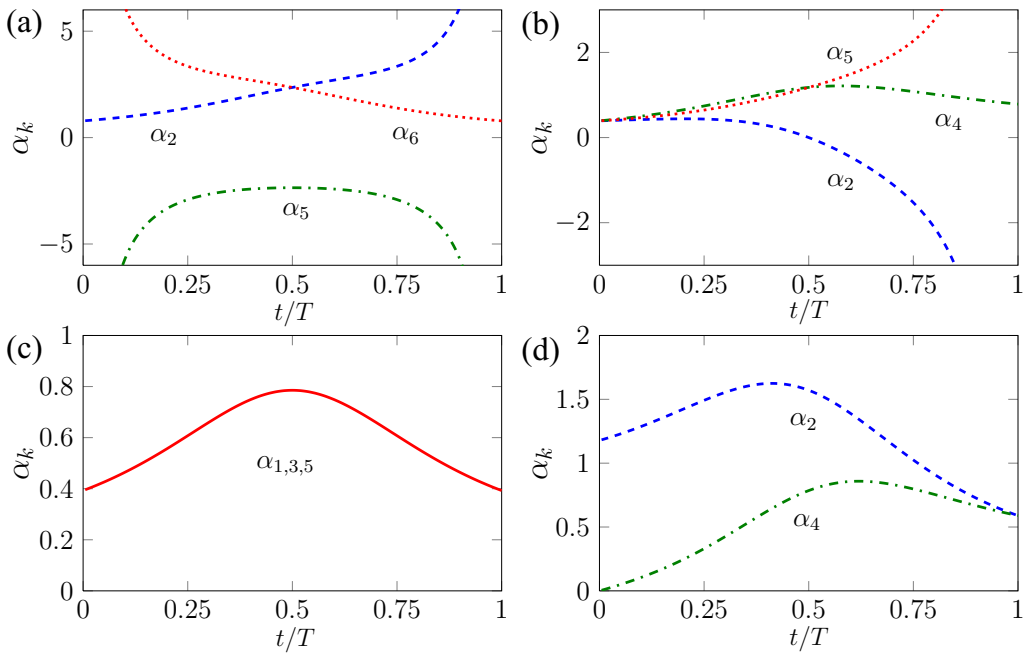

FIG. 1. The time-dependent parameters $\alpha_k(t)$ deduced from the Eqs. (12) on the conditions (a). $\alpha_{1,3,4} = 0$, (b). $\alpha_{1,3,6} = 0$, (c). $\alpha_{2,4,6} = 0$, (d). $\alpha_{1,3,5,6} = 0$, respectively. The corresponding analytical solutions are listed in the Table I.

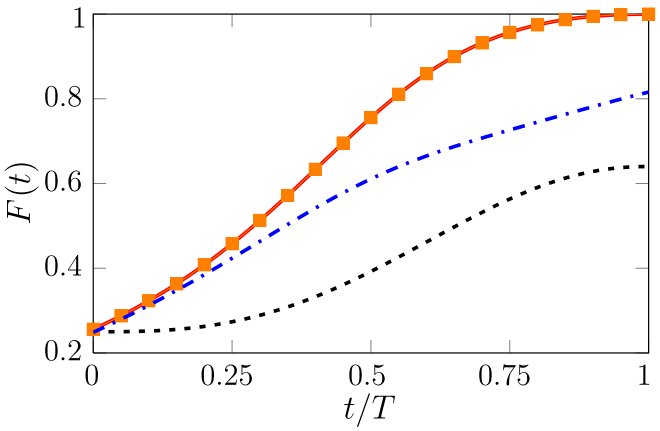

FIG. 2. Quantum state fidelity of the evolved state with different protocols: no additional Hamiltonian (black dashed line), auxiliary Hamiltonian $H'_{add}(t)$ (blue dashed line), additional Hamiltonian $H_{add}(t)$ (orange squares) and exact CD term $H_{cd}(t)$ (red solid line), respectively. Detailed explanation can be found in the main text.

which is less than that in CD protocol (red line), but better than no additional Hamiltonian case (black dashed line). The actual performance is closely related to the time duration T and selected operators h_k. In short, this method offers much flexibility to design speed-up protocols allowed by available resources in experiment.

IV. EXPERIMENT

Our experiment was carried out on a Bruker Avance III 400 MHz (9.4 T) spectrometer equipped with a QXI probe at room temperature. The ensemble of nuclear spins is provided by Diethyl-fluoromalonate dissolved in d-chloroform, where the ^{13}C, ^{1}H, and ^{19}F nuclei constitute a three-spin chain. The molecular structure and relevant properties are given in Fig. 3. The natural Hamiltonian of the three-spin chain in a triple-resonance rotating frame is

$$H_{\rm nmr} = \sum_{i<j,=1}^{3} \frac{\pi J_{ij}}{2} \sigma_z^i \sigma_z^j, \tag{14}$$

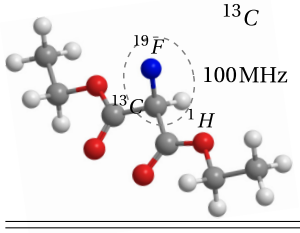

	^{13}C	^{1}H	^{19}F	$T_2(s)$
^{13}C	100 MHz	160.7 Hz	-194.4 Hz	^{13}C 1.1
^{1}H		400 MHz	47.6 Hz	^{1}H 1.2
^{19}F			376 MHz	^{19}F 1.3

FIG. 3. Relevant properties of the natural spin chain consisting of ^{13}C, ^{1}H, ^{19}F nuclear spins marked in the Diethyl-fluoromalonate. The table on the right side summarizes the relevant NMR parameters, i.e., the resonance frequencies ω_i (on the diagonal), the J-coupling constants J_{ij} (above the diagonal), and the relaxation times T_2 in the last columns.

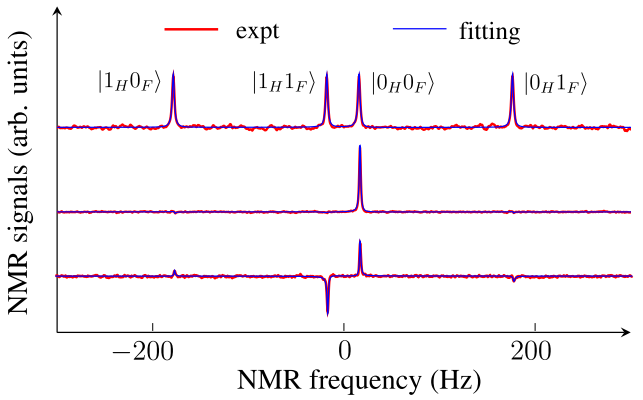

FIG. 4. ^{13}C experimental spectra (red) after a $[\pi/2]_y$ readout pulse applied to carbon channel for equilibrium state (top), PPS (middle), and GHZ state (bottom). The blue spectra show the results by fitting. The four resonance lines are labeled by the corresponding states of the two other qubits.

where J_{ij} represents the coupling strength between spin i and spin j. The experiment consists of the following steps: (i) initial-state preparation; (ii) dynamic evolution along the STA; (iii) quantum measurement and state tomography.

(i) *Initial-state preparation*. Starting from the equilibrium state, we first initialized the system into the pseudopure state (PPS) of the form

$$\rho_{000} = \frac{1-\epsilon}{8}\mathbf{1} + \epsilon|000\rangle\langle 000|$$

through the line-selective pulse method [58], with polarization $\epsilon \approx 10^{-5}$ and $\mathbf{1}$ being the 8×8 identity matrix. The experimental spectrum of the prepared PPS after applying a $[\pi/2]_y$ readout pulse to ^{13}C is shown in Fig. 4. Since we used an unlabeled sample, the information of the ^{1}H and ^{19}F spins was transferred to the ^{13}C spin with a SWAP gate and then the ^{13}C spectra was observed. The prepared PPS was confirmed by a full state tomography [59], which involves the application of seven readout pulses and recording of the spectra of all three channels. The amplitudes of spectra were obtained by a fit to Lorentzians. Figures 6(a) and 6(c) show the reconstructed density matrix $\rho_{\rm exp}^{000}$, from which we calculated the state fidelity to be

$$F = \frac{{\rm Tr}\left(\rho_{\rm exp}^{000}\rho_{\rm th}\right)}{\sqrt{{\rm Tr}\left(\left(\rho_{\rm exp}^{000}\right)^2\right){\rm Tr}\left(\rho_{\rm th}^2\right)}} \approx 0.99, \tag{15}$$

where $\rho_{\rm th}$ is the theoretical density matrix. Then the initial state $[|0\rangle+|1\rangle]^{\otimes 3}$ was produced by applying $[\pi/2]_y$ pulse to the three spins.

(ii) *Dynamic evolution along the STA*. The key step in our experiment is to implement the shortcut to adiabatic passage using $H(t) = H_0(t) + H_{add}(t)$. The evolution operator $U(0,T)$ from time 0 to T is given by

$$U(0,T) = \mathcal{T}\left(e^{-i\int_0^T H(t)dt}\right),$$

where $\mathcal{T}$ denotes the time-ordering operator. For the experimental implementation, the continuous passage was discretized into L segments [60,61], where the step size is chosen such that in the interval $[t_{l-1}, t_l]$ the Hamiltonian $H(t)$ can be

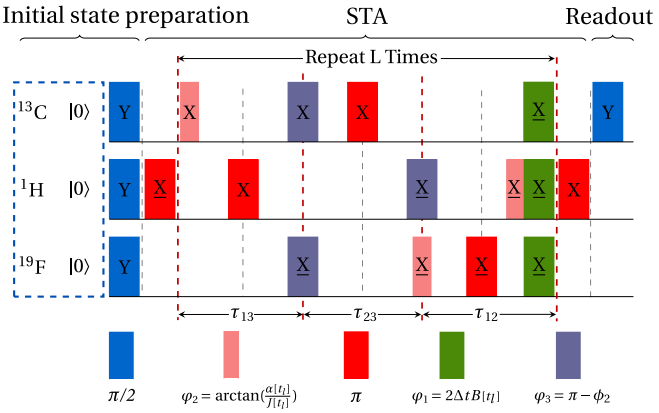

FIG. 5. Pulse sequence in experiments. The color rectangles represent the hard pulses applied to individual qubits and pulse phases is indicated inside them. Time durations $\tau_{12} = \frac{2J[t_l]\Delta t}{\pi J_{12}\cos(\varphi_2)}$, $\tau_{23} = \frac{2J[t_l]\Delta t}{\pi J_{23}\cos(\varphi_2)}$ and $\tau_{13} = \frac{2J[t_l]\Delta t}{\pi |J_{13}|\cos(\varphi_2)}$ represent free evolutions under the natural Hamiltonian.

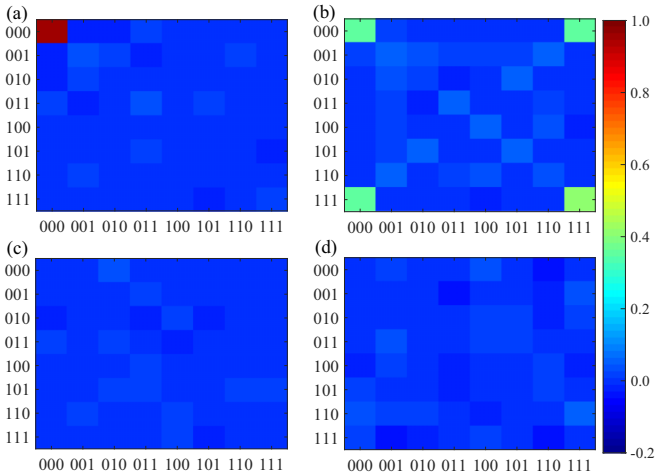

FIG. 6. The real parts (a), (b) and imaginary parts (c), (d) of the experimental density matrices for the initial state $|000\rangle$ (left part), and the GHZ state (right part). The color bar represents the value of density matrix $\rho_{\rm exp}$.

assumed to be constant

$$H[t_l] = -B[t_l]\sum_{i=1}^{3}\sigma_x^i - J[t_l]\sum_{i=1}^{3}\sigma_z^i\sigma_z^{i+1} - \alpha[t_l]\sum_{k=1}^{3}\sigma_z^i\sigma_y^{i+1}$$

with the discrete parameters $B[t_l] = \cos(\pi t_l/(2T))$, $J[t_l] = \sin(\pi t_l/(2T))$, $\alpha[t_l] = \pi/(4T[2-\sin(\pi t_l/T)])$, $t_l = Tl/L = \Delta t l$, and $l = 0, 1 \ldots L$. In the limit of $L \to \infty$ and $\Delta t \to 0$, the total time evolution operator is given by $U(0,T) = \prod_{l=0}^{L} U_l$ with the lth step $U_l = e^{-i\Delta t H[t_l]}$. Though each term of $H[t_l]$ does not commute, U_l can be approximately implemented by the Trotter's formula [62],

$$e^{-i\sum_{j=0}^{3}W_j\Delta t} = \prod_{j=0}^{3}e^{-iW_j\Delta t} + O(\Delta t^2) \tag{16}$$

for arbitrary operators W_j. We here set $W_0 = -B[t_l]\sum_{i=1}^{3}\sigma_x^i$, $W_{j\neq 0} = -J[t_l]\sigma_z^j\sigma_z^{j+1} - \alpha[t_l]\sigma_z^j\sigma_y^{j+1}$ and then the time evolution operator can be expressed as $U_l \approx \prod_{j=0}^{3}e^{-iW_j\Delta t}$. Note that the duration of each step Δt has to be short enough so that the Hamiltonian simulation can have good accuracy. In experiments we chose $L = 7$ and $T = 0.5$, and throughout this process the theoretical fidelity of every step keeps more than 0.993. Each term of U_l can be precisely implemented by a combination of radio-frequency pulses and J-coupling evolutions between the neighboring qubits under NMR pulsing techniques [51,63,64]. As shown in Fig. 5, the shortcut-to-adiabaticity passage can be implemented with the multipulse sequence in experiments.

(iii) *Qutanum measurement and state tomography.* Finally, we performed state tomography on the final states and the reconstructed density matrix $\rho_{\rm exp}$ are shown in Figs. 6(b) and 6(d). To make a quantitative analysis of the results, two measures were adopted: (i) the attenuated correlation [65] defined by

$$c(\rho_{\rm exp}) = \frac{{\rm Tr}(\rho_{\rm th}\rho_{\rm exp})}{{\rm Tr}(\rho_{\rm th}\rho_{\rm th})}, \tag{17}$$

and (ii) the fidelity defined in Eq. (15). The experimental result of the attenuated correlation for the final state was $c(\rho_{\rm exp}) \approx 0.72$ due to the loss of polarization. To remove the effect, we used the second measure and calculated the experimental fidelity to be $F(\rho_{\rm exp}) \approx 0.94$. The imperfections out of the initial-state preparation, radio-frequency pulses, and inhomogeneity of magnetic fields are sources of infidelity. According to our numerical simulations, the imperfection of the initial state produces about 1% error; accumulated deviation of serial pulses produces about 4% error. The experimental time (∼16.9 ms) is short compared to the transverse relaxation time T_2 (∼s), the decoherence caused by the relaxation should be relatively small.

In experiment the instantaneous state fidelity of each step was also calculated to assess the effectiveness of this shortcut. As mentioned, the shortcut-to-adiabaticity passage was discretized into L steps and can be implemented with the multipulse sequence. We experimentally reconstructed density matrix $\rho_{{\rm exp}[t_l]}$ at the lth step by quantum state tomography and calculated the state fidelity defined in Eq. (15) with the instantaneous ground state $\rho_{{\rm th}[t_l]}$ of original Hamiltonian. As shown in Fig. 7, driven by the Hamiltonian $H_0(t) + H_{add}(t)$, the state fidelities keep high throughout the discrete passage (orange x symbols), although a bit lower than the theoretical prediction (black dotted line). This result indicates we have succeeded in constructing a shortcut-to-adiabaticity passage with a simple term $H_{add}(t)$. As a comparison, in experiment the original Hamiltonian $H_0(t)$ was also used to drive the system under the same condition, and the final fidelity dropped to only about 0.35 (blue squares). Note here the continuous passage $H_0(t)$ was also discretized into L steps and the time evolution operator was also approximately implemented with Trotter's formula (the experimental pulse sequence and details can be acquired similarly from Ref. [64]). Therefore, we can conclude that the present scheme can obviously speed up the adiabatic process with feasibility and simplicity in experiment.

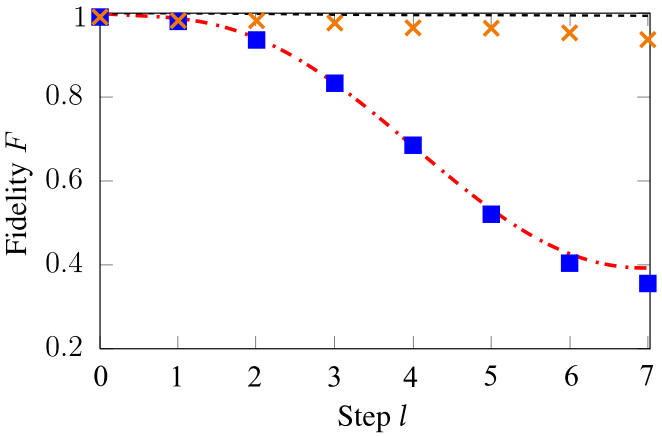

FIG. 7. Instantaneous state fidelity of each step in experiment with original Hamiltonian $H_0(t)$ (blue squares), with Hamiltonian $H_0(t) + H_{add}(t)$ (orange x symbols), respectively. The color dashed lines represent the theoretical expectations with the Trotter's formula for two case. Here, experimental pulse sequence for simulating $H_0(t)$ can be acquired from Ref. [64].

V. CONCLUSIONS AND OUTLOOK

In summary, we prepared a multiparticle entangled state via STA in a three-qubit NMR system. The traditional CD term $H_{cd}(t)$ often takes a complicated form and requires complex resources to realize interactions absent in experiment. To overcome this hurdle, we adopted a flexible method [47], that is, by partially nullifying the nonadiabatic transitions, to create the GHZ state on Ising spin system. This method can significantly reduce the experimental difficulties by decreasing the number of many-body interactions.

Applying the STA protocol in a many-body system is a nontrivial task. This experiment demonstrates the feasibility of this method via current technology and therefore provides an alternative technique to implement fast coherent quantum control in many situations, such as, suppressing the defects produced when crossing a quantum phase transition [39], engineering quantum heat engines [66], and realizing fast quantum information processing for multiqubit systems. Note that in Ref. [45], with a different strategy, the idea of realizing the effective STA by a set of available control terms was also discussed in theory. Recently, by modulating the original Hamiltonian of the system, Petiziol *et al.* [67] also proposed a method for effectively replicating the dynamics of $H_{cd}(t)$ without the need for new unrealizable terms in original Hamiltonian, which also offers a different and feasible method to be investigated in future experiments.

ACKNOWLEDGMENTS

Support came from National Key Research and Development Program of China (Grant No. 2018YFA0306600), National Natural Science Foundation of China (Grants No. 11425523, No. 11661161018, and No. 11605005), Special Funds of the National Natural Science Foundation of China (Grant No. 11847016), and Anhui Initiative in Quantum Information Technologies (Grant No. AHY050000).

[1] A. Ekert and R. Jozsa, Rev. Mod. Phys. **68**, 733 (1996).
[2] C. H. Bennett, G. Brassard, C. Crépeau, R. Jozsa, A. Peres, and W. K. Wootters, Phys. Rev. Lett. **70**, 1895 (1993).
[3] J. Kempe, Phys. Rev. A **60**, 910 (1999).
[4] T. Jennewein, C. Simon, G. Weihs, H. Weinfurter, and A. Zeilinger, Phys. Rev. Lett. **84**, 4729 (2000).
[5] A. Kitaev and J. Preskill, Phys. Rev. Lett. **96**, 110404 (2006).
[6] A. Osterloh, L. Amico, G. Falci, and R. Fazio, Nature (London) **416**, 608 (2002).
[7] X. Wang, A. Bayat, S. Bose, and S. G. Schirmer, Phys. Rev. A **82**, 012330 (2010).
[8] Y. Gao, H. Zhou, D. Zou, X. Peng, and J. Du, Phys. Rev. A **87**, 032335 (2013).
[9] X. Peng, J. Zhang, J. Du, and D. Suter, Phys. Rev. A **77**, 052107 (2008).
[10] S. Dogra, K. Dorai, and Arvind, Phys. Rev. A **91**, 022312 (2015).
[11] P. Král, I. Thanopulos, and M. Shapiro, Rev. Mod. Phys. **79**, 53 (2007).
[12] Y. Zhou, B. Li, X.-X. Li, F.-L. Li, and P.-B. Li, Phys. Rev. A **98**, 052346 (2018).
[13] Y. Lin, J. P. Gaebler, F. Reiter, T. R. Tan, R. Bowler, A. S. Sorensen, D. Leibfried, and D. J. Wineland, Nature (London) **504**, 415 (2013).
[14] X. Q. Shao, J. H. Wu, X. X. Yi, and Gui-Lu Long, Phys. Rev. A **96**, 062315 (2017).
[15] M. Demirplak and S. A. Rice, J. Phys. Chem. A **107**, 9937 (2003); **129**, 154111 (2008).
[16] M. B. Berry, J. Phys. A **42**, 365303 (2009).
[17] A. del Campo, Phys. Rev. Lett. **111**, 100502 (2013).
[18] X. Chen, E. Torrontegui, and J. G. Muga, Phys. Rev. A **83**, 062116 (2011).
[19] X. Chen and J. G. Muga, Phys. Rev. A **86**, 033405 (2012).
[20] S. Masuda and K. Nakamura, Proc. R. Soc. A **466**, 1135 (2010).
[21] E. Torrontegui, S. Martínez-Garaot, A. Ruschhaupt, and J. G. Muga, Phys. Rev. A **86**, 013601 (2012).
[22] S. Ibáñez, S. Martínez-Garaot, X. Chen, E. Torrontegui, and J. G. Muga, Phys. Rev. A **84**, 023415 (2011).
[23] B. T. Torosov, G. Della Valle, and S. Longhi, Phys. Rev. A **87**, 052502 (2013).
[24] G. Vacanti, R. Fazio, S. Montangero, G. M. Palma, M. Paternostro, and V. Vedral, New J. Phys. **16**, 053017 (2014).
[25] J. Jing, M. S. Sarandy, D. A. Lidar, D. W. Luo, and L. A. Wu, Phys. Rev. A **94**, 042131 (2016).
[26] M. Herrera, M. S. Sarandy, E. I. Duzzioni, and R. M. Serra, Phys. Rev. A **89**, 022323 (2014).
[27] J. Zhang, T. H. Kyaw, D. M. Tong, E. Sjoqvist, and L. C. Kwek, Sci. Rep. **5**, 18414 (2015).
[28] T. Wang, Z. Zhang, L. Xiang, Z. Ji, P. Duan *et al.*, New J. Phys. **20**, 065003 (2018).
[29] S. Campbell and S. Deffner, Phys. Rev. Lett. **118**, 100601 (2017).

[30] K. Funo, J.-N. Zhang, C. Chatou, K. Kim, M. Ueda, and A. del Campo, Phys. Rev. Lett. **118**, 100602 (2017).
[31] Y. X. Du, Z. T. Liang, Y. C. Li, X. X. Yue, Q. X. Lv, W. Huang, X. Chen, H. Yan, and S. L. Zhu, Nature Commun. **7**, 12479 (2016).
[32] S. An, D. Lv, A. del Campo, and K. Kim, Nature Commun. **7**, 12999 (2016).
[33] M. Okuyama and K. Takahashi, Phys. Rev. Lett. **117**, 070401 (2016).
[34] B. B. Zhou, A. Baksic, H. Ribeiro, C. G. Yale, F. J. Heremans, P. C. Jerger, A. Auer, G. Burkard, A. A. Clerk, and D. D. Awschalom, Nature Phys. **13**, 330 (2017).
[35] K. Takahashi, New J. Phys. **19**, 115007 (2017).
[36] T. H. Kyaw and L.-C. Kwek, New J. Phys. **20**, 045007 (2018).
[37] T. Hatomura, New J. Phys. **20**, 015010 (2018).
[38] F. Kleißler, A. Lazariev, and S. Arroyo-Camejo, NPJ Quantum. Inf. **4**, 49 (2018).
[39] A. del Campo, M. M. Rams, and W. H. Zurek, Phys. Rev. Lett. **109**, 115703 (2012).
[40] S. Ibáñez, X. Chen, E. Torrontegui, J. G. Muga, and A. Ruschhaupt, Phys. Rev. Lett. **109**, 100403 (2012).
[41] K. Takahashi, Phys. Rev. E **87**, 062117 (2013).
[42] D. Sels and A. Polkovnikov, Proc. Natl. Acad. Sci. USA **114**, E3909 (2017).
[43] S. Ibáñez, X. Chen, and J. G. Muga, Phys. Rev. A **87**, 043402 (2013).
[44] S. Martínez-Garaot, E. Torrontegui, X. Chen, and J. G. Muga, Phys. Rev. A **89**, 053408 (2014).
[45] T. Opatrný and K. Mølmer, New J. Phys. **16**, 015025 (2014).
[46] Y. H. Chen, Y. Xia, Q. Q. Chen, and J. Song, Sci. Rep. **5**, 15616 (2015).
[47] Y. H. Chen, Y. Xia, Q. C. Wu, B. H. Huang, and J. Song, Phys. Rev. A **93**, 052109 (2016).
[48] V. Giovannetti, S. Lloyd, and L. Maccone, Science **306**, 1330 (2004).
[49] T. Monz, P. Schindler, J. T. Barreiro, M. Chwalla, D. Nigg, W. A. Coish, M. Harlander, W. Hänsel, M. Hennrich, and R. Blatt, Phys. Rev. Lett. **106**, 130506 (2011).
[50] D. Jaksch, C. Bruder, J. I. Cirac, C. W. Gardiner, and P. Zoller, Phys. Rev. Lett. **81**, 3108 (1998).
[51] L. M. K. Vandersypen and I. L. Chuang, Rev. Mod. Phys. **76**, 1037 (2005).
[52] X.-L. Deng, D. Porras, and J. I. Cirac, Phys. Rev. A **72**, 063407 (2005).
[53] M. D. Bowdrey, J. A. Jones, E. Knill, and R. Laflamme, Phys. Rev. A **72**, 032315 (2005).
[54] J. Li, R. Fan, H. Wang, B. Ye, B. Zeng, H. Zhai, X. Peng, and J. Du, Phys. Rev. X **7**, 031011 (2017).
[55] J. Zhang, G. Pagano, P. W. Hess, A. Kyprianidis, P. Becker, H. Kaplan, A. V. Gorshkov, Z. X. Gong, and C. Monroe, Nature (London) **551**, 601 (2017).
[56] J. Zeiher, J. Y. Choi, A. Rubio-Abadal, T. Pohl, R. M. W. van Bijnen, I. Bloch, and C. Gross, Phys. Rev. X **7**, 041063 (2017).
[57] C. H. Tseng, S. Somaroo, Y. Sharf, E. Knill, R. Laflamme, T. F. Havel, and D. G. Cory, Phys. Rev. A **61**, 012302 (1999).
[58] X. Peng, X. Zhu, X. Fang, M. Feng, K. Gao, X. Yang, and M. Liu, Chem. Phys. Lett. **340**, 509 (2001).
[59] J.-S. Lee, Phys. Lett. A **305**, 349 (2002).
[60] X. Peng, S. Wu, J. Li, D. Suter, and J. Du, Phys. Rev. Lett. **105**, 240405 (2010).
[61] N. Xu, J. Zhu, D. Lu, X. Zhou, X. Peng, and J. Du, Phys. Rev. Lett. **108**, 130501 (2012).
[62] M. Suzuki, Proc. Jpn. Acad. Ser. B **69**, 161 (1993).
[63] R. Somma, G. Ortiz, J. E. Gubernatis, E. Knill, and R. Laflamme, Phys. Rev. A **65**, 042323 (2002).
[64] X. Peng, J. F. Zhang, J. F. Du, and D. Suter, Phys. Rev. Lett. **103**, 140501 (2009).
[65] G. Teklemariam, E. M. Fortunato, M. A. Pravia, T. F. Havel, and D. G. Cory, Phys. Rev. Lett. **86**, 5845 (2001).
[66] A. del Campo, J. Goold, and M. Paternostro, Sci. Rep. **4**, 6208 (2014).
[67] F. Petiziol, B. Dive, F. Mintert, and S. Wimberger, Phys. Rev. A **98**, 043436 (2018).